Electronic Supplementary Material (ESI) for Physical Chemistry Chemical Physics.

Fluorine Conformational Effects Characterized by Energy Decomposition Analysis

Natalia Díaz*, Fernando Jiménez-Grávalos, Dimas Suárez, Evelio Francisco, and Angel Martín-Pendás

Departamento de Química Física y Analítica. Universidad de Oviedo. Avda. Julián Clavería 8, 33006 Oviedo (Asturias). Spain.

diazfnatalia@uniovi.es

ELECTRONIC SUPPLEMENTARY INFORMATION

Table S1. IQA energy components at the HF-D3/cc-pVTZ (sum for all the atoms and interatomic interactions) for the energy difference (kcal/mol) between the two conformers (gauche/anti or trans/cis) in 1,2-difluoroethane and related small systems.

$\Delta E = E_{gauche} - E_{anti}$	ΔE_{net}	$\Delta E_{int,disp}$	$\Delta E_{int,xc}$	$\Delta E_{int,class}$	ΔE_{IQA}
1: 1,2-difluoroethane	3.7	-0.1	-1.9	-2.3	-0.5
2: 2-fluoroethyl-acetate	0.2	-0.1	-2.2	1.6	-0.5
3: 3-fluoropropanal	-10.9	-0.0	0.9	8.9	-1.2
4: *N*-(2-fluoroethyl)acetamide	-24.6	-0.3	-2.3	25.0	-2.1
5: 2-(2-fluoroethyl)isoindoline-1,3-dione	-0.3	-0.3	-2.2	2.3	-0.5
6: 2-fluoroethan-1-aminium	-24.8	-0.6	1.9	16.2	-7.3
7: 1-(2-fluoroethyl)pyridin-1-ium	-20.4	-0.4	-0.8	16.5	-5.1
$\Delta E = E_{trans} - E_{cis}$	ΔE_{net}	$\Delta E_{int,disp}$	$\Delta E_{int,xc}$	$\Delta E_{int,class}$	ΔE_{IQA}
8: 1-fluoropropan-2-one	-30.8	-0.0	5.0	23.1	-2.7
9: methyl-2-fluoroacetate	2.1	-0.0	1.4	-3.5	0.0
10: 2-fluoro-*N*-methylacetamide	-4.8	-0.2	8.7	-9.5	-5.8

Table S2. Largest differences in the atomic energies (kcal/mol) between the gauche and anti F_2-C_1-C_5-X conformers in CH_2F-CH_2X systems ($\Delta E = E_{gauche} - E_{anti}$). Ball-and-stick models of the gauche conformer including atom numbering.

$\Delta E = E_{gauche} - E_{anti}$	ΔE_{net}		$\Delta E^{AB}_{\text{int,clas}}$		$\Delta E^{AB}_{\text{int,xc}}$	
1: 1,2-difluoroethane 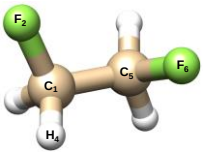	F_2	1.1	$F_2\cdots F_6$	12.1	$C_1\cdots C_5$	-3.2
	F_6	1.0	$C_1\cdots F_6$	-8.0	$C_1\cdots F_6$	1.0
	C_1	1.0	$F_2\cdots C_5$	-7.9	$F_2\cdots C_5$	1.0
			$C_1\cdots C_5$	6.9	$F_2\cdots F_6$	-0.9
					$C_1\cdots H_4$	0.8
					$C_5\cdots H_8$	0.8
2: 2-fluoroethyl-acetate 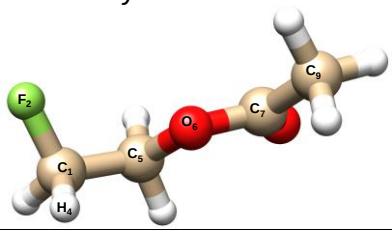	O_6	1.3	$F_2\cdots O_6$	20.8	$C_1\cdots C_5$	-3.0
			$F_2\cdots C_7$	-14.0	$F_2\cdots O_6$	-1.6
			$C_1\cdots O_6$	-11.9	$C_1\cdots O_6$	1.2
			$C_1\cdots C_7$	7.6	$F_2\cdots C_5$	1.0
			$F_2\cdots C_5$	-7.6	$C_7\cdots O_8$	0.9
					$O_6\cdots C_7$	-0.9
3: 3-fluoropropanal 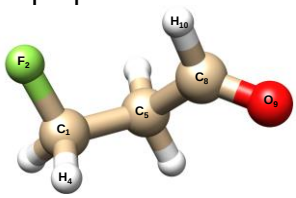	C_1	-6.9	$F_2\cdots C_8$	-15.9	$F_2\cdots H_{10}$	-1.7
			$F_2\cdots O_9$	11.8	$C_1\cdots F_2$	1.0
			$C_8\cdots H_{10}$	7.4	$C_1\cdots C_5$	-1.0
			$C_1\cdots F_2$	6.5	$C_8\cdots O_9$	0.9
			$O_9\cdots H_{10}$	-5.7	$F_2\cdots C_8$	-0.9
			$C_1\cdots C_8$	5.6	$C_1\cdots C_8$	0.8
					$C_8\cdots H_{10}$	-0.7
4: *N*-(2-fluoroethyl)acetamide 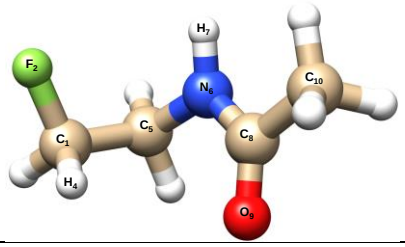	N_6	-8.2	$F_2\cdots N_6$	27.9	$F_2\cdots N_6$	-2.5
	C_1	-7.6	$F_2\cdots C_8$	-16.5	$H_3\cdots O_9$	2.4
			$N_6\cdots C_8$	13.3	$C_1\cdots C_5$	-2.2
			$F_2\cdots H_7$	-12.8	$H_4\cdots O_9$	-1.7
					$C_1\cdots F_2$	1.3
					$C_5\cdots N_6$	-1.2
5: 2-(fluoroethyl)isoindoline-1,3-dione 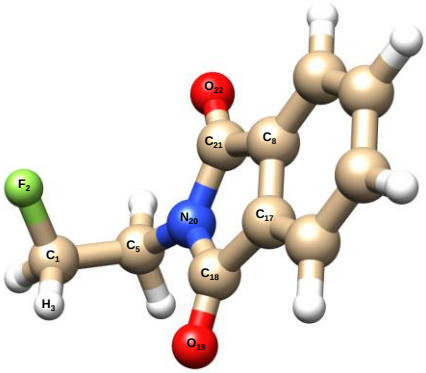	C_1	-3.9	$F_2\cdots C_{21}$	-32.4	$H_3\cdots O_{19}$	-2.6
	C_{21}	3.7	$F_2\cdots N_{20}$	32.2	$F_2\cdots N_{20}$	-2.5
			$F_2\cdots C_{18}$	-23.8	$C_1\cdots C_5$	-1.7
			$F_2\cdots O_{22}$	19.9	$C_1\cdots N_{20}$	1.6
			$C_1\cdots N_{20}$	-17.0	$C_{18}\cdots O_{19}$	1.5

Table S2 (cont.)

6: 2-fluoroethan-1-aminium 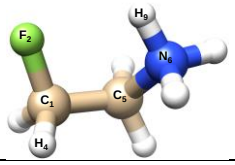	C_1	-28.2	$F_2\cdots N_6$ $F_2\cdots H_9$ $C_1\cdots F_2$ $N_6\cdots H_9$ $C_1\cdots H_9$	32.2 -26.6 25.0 -15.2 13.0	$N_6\cdots H_9$ $C_1\cdots F_2$ $F_2\cdots N_6$ $C_1\cdots C_5$ $F_2\cdots H_9$	6.6 4.8 -4.4 -3.1 -2.4
7: 1-(2-fluoroethyl)pyridine-1-ium 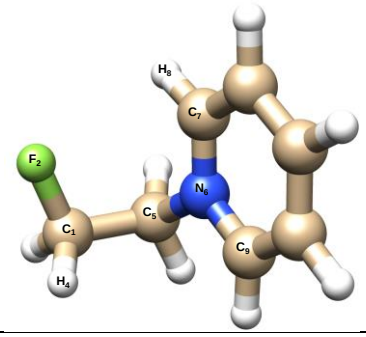	C_1	-17.7	$F_2\cdots N_6$ $F_2\cdots C_7$ $C_1\cdots F_2$ $C_1\cdots N_6$	34.3 16.7 14.6 -11.5	$C_1\cdots F_2$ $C_1\cdots C_5$ $F_2\cdots C_7$ $F_2\cdots N_6$	3.0 -2.9 -2.3 -2.2

Table S3. Largest differences in the atomic energies (kcal/mol) between the F_2-C_1-C_5=O_6 *trans* and *cis* conformers in CH_2F-COX systems ($\Delta E = E_{trans} - E_{cis}$). Ball-and-stick models for the trans conformers including atom numbering.

$\Delta E = E_{trans} - E_{cis}$	ΔE_{net}		$\Delta E^{AB}_{\text{int,clas}}$		$\Delta E^{AB}_{\text{int,xc}}$	
8: 1-fluoropropan-2-one 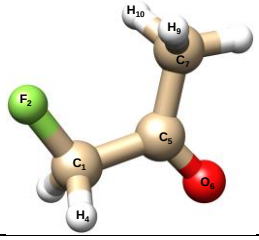	C_1	-17.2	$C_1 \cdots C_5$	-26.4	$F_2 \cdots O_6$	4.5
	C_5	-10.3	$C_1 \cdots O_6$	24.9	$F_2 \cdots C_7$	-3.1
	F_2	-5.2	$F_2 \cdots O_6$	-23.9	$C_1 \cdots O_6$	-3.0
			$F_2 \cdots C_5$	19.1	$C_1 \cdots F_2$	3.0
			$C_1 \cdots F_2$	17.6	$C_5 \cdots O_6$	3.0
					$C_1 \cdots C_5$	2.5
					$C_5 \cdots C_7$	-2.5
9: methyl-2-fluoroacetate 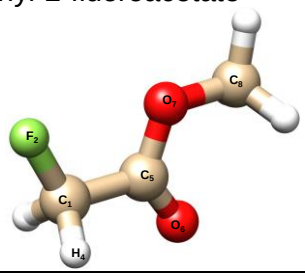	C_5	5.4	$F_2 \cdots O_7$	27.9	$F_2 \cdots O_7$	-5.2
	C_1	-5.0	$F_2 \cdots O_6$	-25.2	$C_5 \cdots O_6$	4.6
	O_7	4.9	$C_1 \cdots O_6$	18.2	$F_2 \cdots O_6$	4.2
			$C_1 \cdots O_7$	-14.7	$C_5 \cdots O_7$	-4.0
			$C_5 \cdots O_7$	-12.9	$C_1 \cdots O_7$	3.2
			$F_2 \cdots C_8$	-8.2	$C_1 \cdots O_6$	-2.9
10: 2-fluoro-*N*-methylacetamide 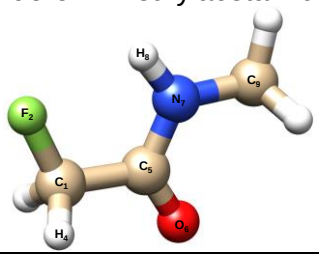	C_1	-23.5	$F_2 \cdots N_7$	39.6	$N_7 \cdots H_8$	8.3
	N_7	15.5	$C_1 \cdots O_6$	28.6	$C_5 \cdots N_7$	-5.8
	H_8	9.1	$F_2 \cdots O_6$	-25.1	$F_2 \cdots N_7$	-5.3
	F_2	-6.9	$N_7 \cdots H_8$	-24.4	$C_5 \cdots O_6$	5.1
			$F_2 \cdots H_8$	-24.4	$F_2 \cdots O_6$	4.7
			$C_5 \cdots N_7$	-24.0	$C_1 \cdots F_2$	4.7
			$C_1 \cdots F_2$	23.4	$C_1 \cdots O_6$	-3.1
			$C_1 \cdots C_5$	-21.0	$F_2 \cdots H_8$	-3.0

Table S4. Largest differences in the atomic energies (kcal/mol) between the *g+/g+* conformer of 1,2,3-trifluoropropane (**11** in Scheme 1) and the rest of conformers ($\Delta E = E_{g+/g+} - E_i$). Ball-and-stick models for the *i*-conformers including atom numbering.

$\Delta E = E_{g+/g+} - E_i$	ΔE_{net}		$\Delta E^{AB}_{\text{int,clas}}$		$\Delta E^{AB}_{\text{int,xc}}$	
g+/g- 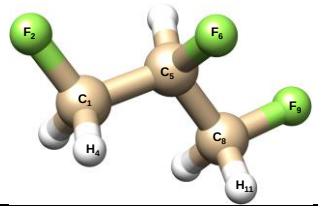	C_8	-6.4	$C_1\cdots F_9$	-11.4	$C_1\cdots F_9$	-1.9
	C_1	-2.6	$F_2\cdots F_9$	6.7	$H_4\cdots F_9$	-1.7
			$C_8\cdots H_{10}$	6.4	$C_8\cdots F_9$	1.2
			$C_8\cdots F_9$	6.3	$H_3\cdots H_{10}$	1.0
g+/anti 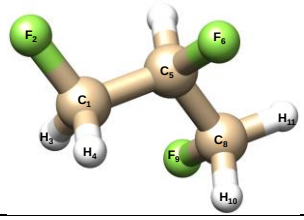	H_3	-1.4	$F_6\cdots F_9$	11.6	$C_5\cdots C_8$	-2.8
	H_4	1.4	$C_5\cdots F_9$	-7.5	$H_3\cdots F_9$	1.9
			$F_6\cdots C_8$	-7.4	$H_4\cdots F_9$	-1.6
					$C_1\cdots C_5$	1.3
g-/g+ 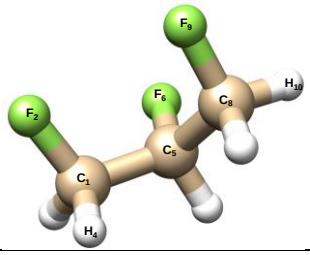	C_8	-12.1	$F_2\cdots C_8$	19.2	$F_2\cdots F_9$	3.6
	C_1	-8.1	$F_2\cdots F_9$	-19.1	$C_8\cdots F_9$	2.1
	F_2	-5.1	$C_1\cdots C_8$	-14.2	$C_1\cdots F_9$	-1.9
	F_9	-4.7	$C_8\cdots F_9$	12.2	$C_1\cdots F_2$	1.8
			$C_1\cdots F_9$	10.5	$H_4\cdots F_9$	-1.7
			$C_1\cdots H_4$	9.3		
g-/anti 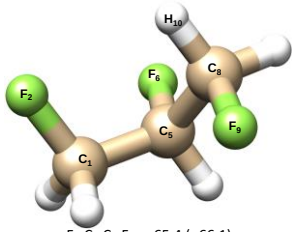	C_1	4.1	$F_2\cdots C_8$	13.0	$C_5\cdots C_8$	-3.2
			$F_6\cdots F_9$	11.6	$F_2\cdots H_{10}$	2.3
			$F_2\cdots F_9$	-11.1	$F_2\cdots C_8$	1.5
			$C_5\cdots F_9$	-7.6	$C_1\cdots C_5$	1.3
			$F_6\cdots C_8$	-6.8		
anti/anti 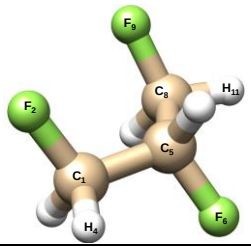	C_8	-8.1	$F_2\cdots F_9$	-17.5	$C_5\cdots C_8$	-2.76
	C_5	4.4	$F_2\cdots C_8$	16.7	$F_2\cdots F_9$	2.56
	C_1	-3.8	$F_2\cdots F_6$	12.8	$C_1\cdots F_9$	-2.02
			$F_6\cdots F_9$	11.9	$H_4\cdots F_9$	-1.69
			$C_1\cdots C_8$	-10.1	$C_1\cdots C_5$	-1.67
			$F_2\cdots C_5$	-9.7		

Table S5. Largest differences in the atomic energies (kcal/mol) between the **g+/trans** conformer of 2,3-difluoro-*N*-methylpropanamide (**12** in Scheme 1) and the rest of conformers ($\Delta E = E_{g+/trans} - E_i$). Ball-and-stick models for the *i*-conformers including atom numbering.

$\Delta E = E_{g+/trans} - E_i$	ΔE_{net}	$\Delta E_{\mathrm{int,clas}}^{A\cdots B}$	$\Delta E_{\mathrm{int,xc}}^{A\cdots B}$
g-/trans 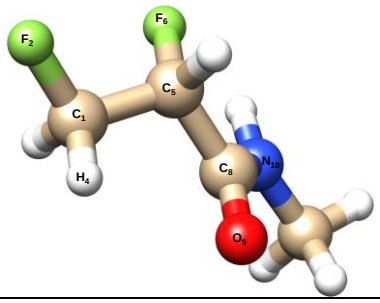	C_8 9.4	$F_2\cdots C_8$ -38.4 $F_2\cdots N_{10}$ 29.8 $C_1\cdots C_8$ 22.9 $F_2\cdots O_9$ 21.4 $C_1\cdots N_{10}$ -15.8	$H_4\cdots O_9$ 3.1 $H_3\cdots O_9$ -2.0 $F_2\cdots C_8$ -1.0 $C_5\cdots C_8$ 1.0
anti/trans 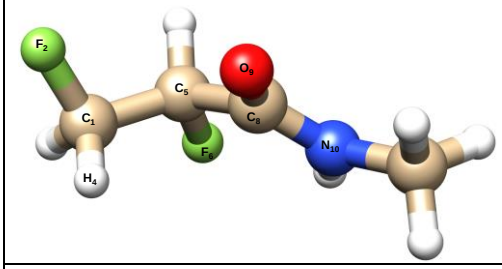	C_1 -10.6 C_8 5.4	$F_2\cdots N_{10}$ 25.9 $F_2\cdots C_8$ -16.2 $F_2\cdots F_6$ 13.4	$C_1\cdots C_5$ -4.0 $H_3\cdots O_9$ -2.1 $H_3\cdots F_6$ 1.8 $C_1\cdots F_2$ 1.8 $C_8\cdots N_{10}$ -1.6
g+/cis 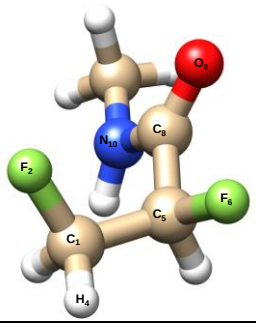	N_{10} 19.9 C_5 -19.4 H_{11} 10.0 C_1 -8.0	$F_6\cdots N_{10}$ 40.2 $C_8\cdots N_{10}$ -32.9 $N_{10}\cdots H_{12}$ -28.2 $C_5\cdots O_9$ 28.0	$N_{10}\cdots H_{11}$ 9.2 $C_8\cdots N_{10}$ -7.5 $C_8\cdots O_9$ 7.0 $F_6\cdots N_{10}$ -5.5 $F_6\cdots O_9$ 5.2 $C_5\cdots F_6$ 4.3
anti/cis 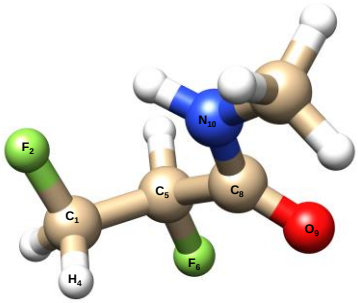	C_5 -17.3 C_1 7.5	$F_6\cdots N_{10}$ 37.6 $C_5\cdots O_9$ 28.9 $C_1\cdots O_9$ -28.6 $F_6\cdots O_9$ -27.1	$F_6\cdots O_9$ 5.7 $F_6\cdots N_{10}$ -5.5 $C_8\cdots O_9$ 5.0 $C_8\cdots N_{10}$ -4.5 $C_5\cdots F_6$ 4.1 $F_2\cdots H_{11}$ 3.7 $C_1\cdots C_5$ -3.4

IQF analysis of fragments from an α,β-difluoro-γ-amino-acid

Figure S1. Ball-and-stick representation of the nine conformers optimized for 2-(2,3-difluoropropyl)isoindoline-1,3-dione (**13** in Scheme 1). F-C-C-F and F-C-C-N dihedral angles (º) and selected interatomic distances (Å) measured in the HF-D3/cc-pVTZ optimized structures (RI-MP2/cc-pVTZ in parentheses) are included. Energy differences ($E_{g+/g+} - E_i$) in kcal/mol computed at the HF-D3/cc-pVTZ, RI-MP2/cc-pVTZ (in parentheses) and DLPNO-CCSD(T)/aug-cc-pVTZ [in brackets] levels of theory are also included.

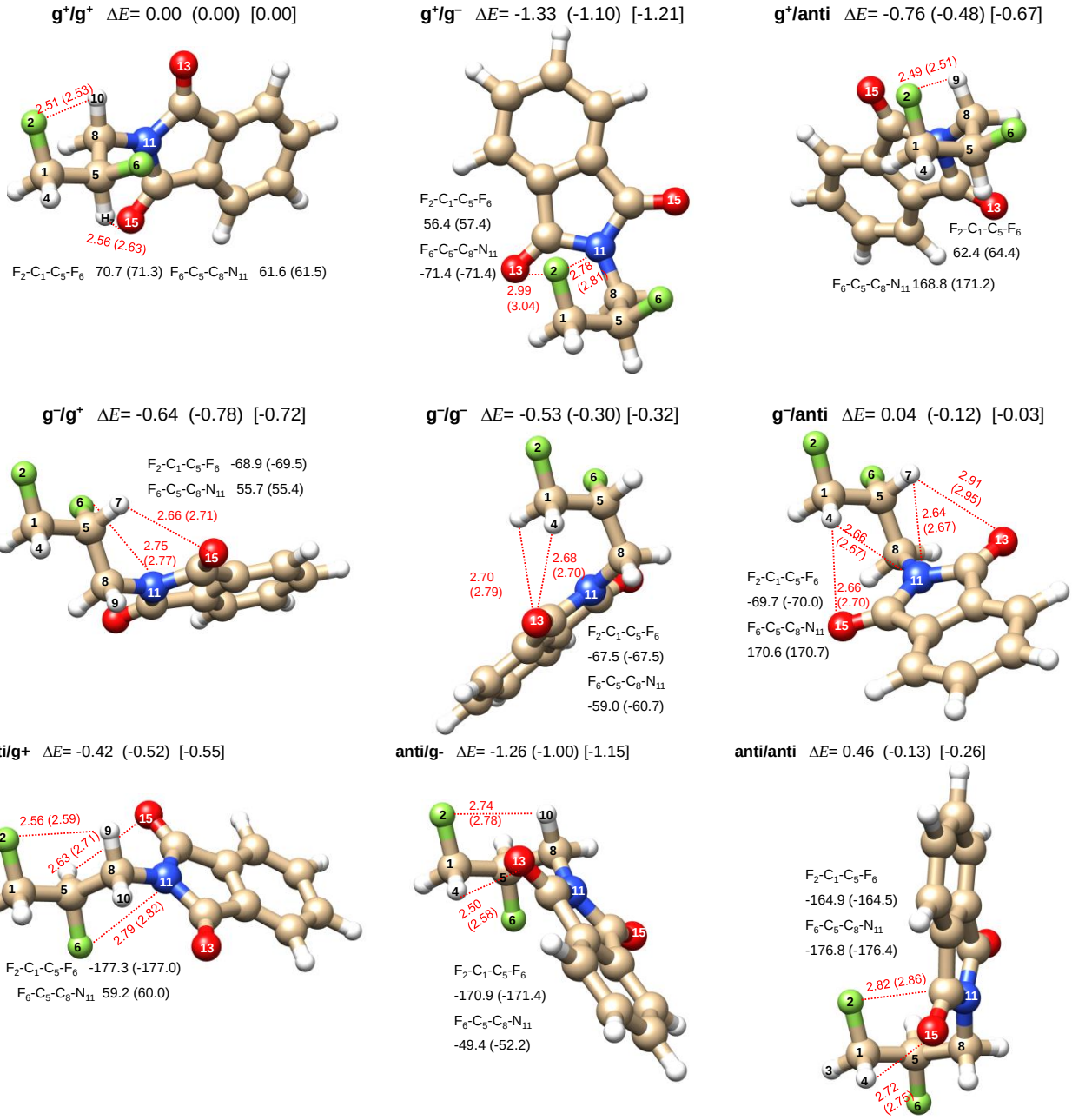

Table S6. IQF energy components at the HF-D3/cc-pVTZ level (in kcal/mol) for the energy differences among the nine conformers optimized for 2-(2,3-difluoropropyl)isoindoline-1,3-dione (**13**). A three-fragment partitioning scheme (P=CH_2F, Q=CHF, and R=CH_2isoindoline-1,3-dione) is assumed for the different conformers. Relative energies are given as $E_{g+/g+} - E_i$, so that a negative value means further stabilization of *g+/g+*.

	ΔE^P_{net}	ΔE^Q_{net}	ΔE^R_{net}	$\Delta E_{int,disp}$			$\Delta E_{int,xc}$			$\Delta E_{int,class}$			ΔE_{IQA}	$\Delta E_{HF\text{-}D3}$
				$P\cdots Q$	$P\cdots R$	$Q\cdots R$	$P\cdots Q$	$P\cdots R$	$Q\cdots R$	$P\cdots Q$	$P\cdots R$	$Q\cdots R$		
$\Delta E = E_{g+/g+} - E_{g+/g-}$	-7.2	3.1	-4.5	0.1,	2.3,	-1.1	-0.7,	8.6,	-4.4	0.1,	1.6,	-0.2	-2.2	-1.3
$\Delta E = E_{g+/g+} - E_{g+/anti}$	-2.3	2.1	0.2	0.0,	1.3,	-0.6	-0.0,	3.4,	-3.9	-0.2,	-0.9,	0.0	-1.1	-0.8
$\Delta E = E_{g+/g+} - E_{g-/g+}$	0.8	-1.5	1.8	0.0,	-0.1,	-0.1	0.3,	-1.4,	-0.4	-0.8,	-0.4,	0.0	-1.7	-0.6
$\Delta E = E_{g+/g+} - E_{g-/g-}$	-5.9	2.4	1.0	0.1,	1.8,	-1.0	0.4,	5.1,	-3.5	-0.3,	0.2,	-0.3	-0.1	-0.5
$\Delta E = E_{g+/g+} - E_{g-/anti}$	-3.8	1.6	1.7	0.0,	1.6,	-0.9	0.5,	3.7,	-4.6	-0.5,	-0.0,	0.0	-0.7	0.0
$\Delta E = E_{g+/g+} - E_{anti/g+}$	0.5	0.1	0.7	0.0,	-0.0,	-0.1	-2.4,	-0.4,	0.1	1.6,	-0.4,	-0.5	-0.9	-0.4
$\Delta E = E_{g+/g+} - E_{anti/g-}$	-4.4	2.1	-1.4	0.1,	1.6,	-0.9	-1.9,	5.2,	-3.1	2.0,	-0.8,	-0.4	-1.9	-1.3
$\Delta E = E_{g+/g+} - E_{anti/anti}$	-4.7	1.7	-2.7	0.0,	2.3,	-0.8	-2.8,	7.0,	-4.0	2.2,	1.7,	-0.3	-0.3	0.5

The optimized conformers for **13** alternate *gauche* (*g+* and *g-*) and *anti* orientations in the adjacent F_2-C_1-C_5-F_6 and F_6-C_5-C_8-N_{11} groups and remain quite close in energy (< 1.2 kcal/mol). The *gauche* effect between vicinal F atoms is reflected in favorable exchange-correlation and unfavorable electrostatic inter-fragment interactions ($\Delta E^{P\cdots Q}_{\text{int},xc}$=-2.4 kcal/mol and $\Delta E^{P\cdots Q}_{\text{int,class}}$=1.6 kcal/mol for the *anti/g+* conformer; see also *anti/g-* and *anti*/*anti* in Table S6). Most likely, this determines the relative stability of the *anti/g+* conformer with respect to *g+/g+* (ΔE^{IQA}=–0.9 kcal/mol). Actually, the similar stability of all the conformers indicates that the placement of the bulky –CH_2-isoindole-1,3-dione group (fragment R) induces little or none conformational effects. This is not entirely unexpected because the presence of the vicinal methylene group and the relatively large size and *symmetric* structure of the isoindole moiety can yield similar $P\cdots R$ and $Q\cdots R$ interactions with the smaller P=CH_2F and Q=CHF fragments across the various conformers. This observation is not incompatible with the fact that the net and inter-fragment IQF energies (and the underlying atomic contributions) involving fragment R vary significantly upon conformational change. For example, on going from the extended *g+/g+* reference to the more compact *g+/g-* and *anti*/*anti* conformers, the closer $Q\cdots R$ contacts in *g+/g+* are replaced by the $P\cdots R$ ones. These structural changes leave a mark on the $\Delta E^{P\cdots R}_{\text{int},xc}$ values of 8.6 and 7.0 kcal/mol for *g+/g-* and *anti/anti*, respectively, and on the $\Delta E^{Q\cdots R}_{\text{int},xc}$ ones of -4.4 and -4.0 kcal/mol. Parallel energy variations of 2.3 and -1.0 kcal/mol arise in the dispersion $\Delta E^{P\cdots R}_{\text{int},disp}$ and $\Delta E^{Q\cdots R}_{\text{int},disp}$ terms. The $P\cdots R$ and $Q\cdots R$ interactions are also concomitant with opposite changes in the net fragment energies ($\Delta E^P_{\text{net}} + \Delta E^Q_{\text{net}} + \Delta E^R_{\text{net}}$ = -8.6 and -5.7 kcal/mol for *g+/g-* and *anti*/*anti*).

Table S7. Largest differences in the atomic energies (kcal/mol) between the **g+/g+** conformer of 2-(2,3-difluoropropyl)isoindoline-1,3-dione (**13** in Scheme 1) and the rest of conformers ($\Delta E = E_{g+/g+} - E_i$). Ball-and-stick models for the *i*-conformers including atom numbering.

$\Delta E = E_{g+/g+} - E_i$	ΔE_{net}	$\Delta E^{AB}_{\text{int,clas}}$	$\Delta E^{AB}_{\text{int,xc}}$
g+/g- 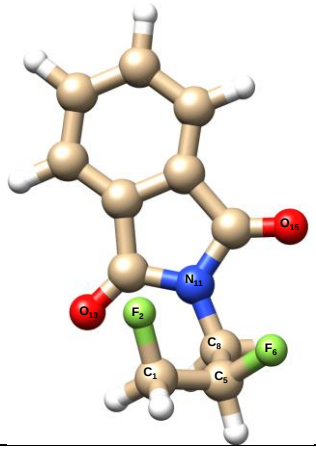	C_{14} -6.8 C_5 -5.4 F_2 -4.2	$F_2\cdots C_{12}$ 69.9 $C_1\cdots C_{12}$ -57.8 $F_2\cdots N_{11}$ -51.3 $F_2\cdots O_{13}$ -48.9 $C_1\cdots O_{13}$ 44.3	$F_2\cdots N_{11}$ 4.7 $C_{12}\cdots O_{13}$ -3.8
g+/anti 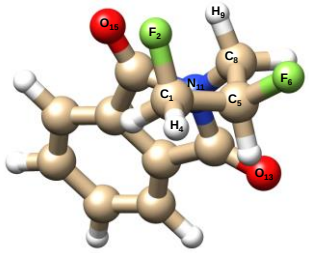	C_{12} 7.0 C_1 -3.8 C_5 -3.6 C_8 3.3	$F_2\cdots C_{14}$ 36.2 $C_1\cdots C_{14}$ -35.0 $F_6\cdots N_{11}$ 32.8 $F_2\cdots O_{15}$ -32.6	$C_{14}\cdots O_{15}$ 3.4 $H_7\cdots O_{15}$ -3.1
g-/g+ 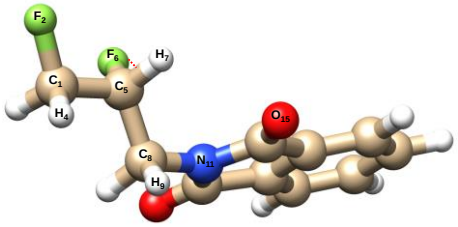	C_1 -4.7	$F_2\cdots C_{12}$ -13.8 $F_2\cdots N_{11}$ 11.9 $F_2\cdots O_{13}$ 11.5	$F_2\cdots H_{10}$ -2.0 $F_2\cdots C_8$ -1.9
g-/g- 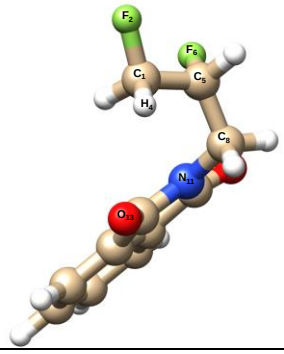	C_{12} 7.0 H_{10} 3.2 N_{11} 3.2	$C_1\cdots C_{12}$ -29.8 $C_1\cdots O_{13}$ 28.2 $F_6\cdots C_{12}$ -16.4	$C_{14}\cdots O_{15}$ 3.9 $N_{11}\cdots C_{14}$ -3.6 $C_{12}\cdots O_{13}$ -3.3 $H_7\cdots O_{15}$ -3.1

g-/anti 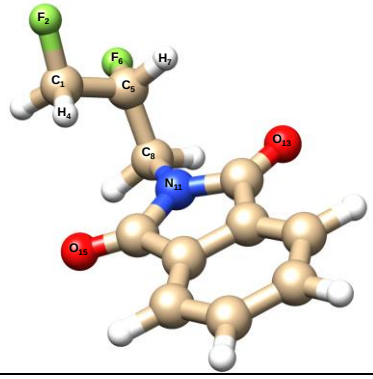	C_{12} 6.0 H_4 -3.0	$F_6\cdots N_{11}$ 32.8 $F_6\cdots C_{12}$ -29.5 $F_6\cdots C_{14}$ -28.2 $C_1\cdots C_{14}$ -23.8	$H_7\cdots O_{15}$ -3.1 $F_6\cdots N_{11}$ -2.6 $H_4\cdots O_{15}$ 2.5
anti/g+ 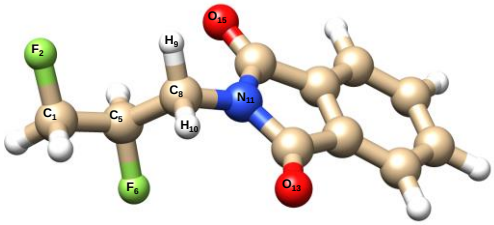	C_{14} -2.0 H_{10} 1.7	$F_2\cdots F_6$ 11.9 $F_2\cdots O_{15}$ -9.4 $F_2\cdots O_{13}$ 8.2 $F_2\cdots C_{14}$ 8.0 $F_2\cdots C_{12}$ -7.9	$C_1\cdots C_5$ -2.8 $F_2\cdots H_{10}$ -2.0 $F_2\cdots H_9$ 1.8
anti/g- 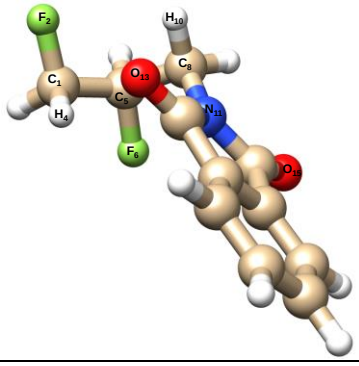	N_{11} 6.4 C_{12} 4.7 C_5 -4.0	$C_1\cdots C_{12}$ -37.7 $C_1\cdots O_{13}$ 36.1 $F_2\cdots O_{13}$ -31.3 $F_2\cdots C_{12}$ 30.3	$H_4\cdots O_{13}$ 3.6 $C_{14}\cdots O_{15}$ 3.4 $C_1\cdots C_5$ -3.2 $H_7\cdots O_{15}$ -3.1
anti/anti 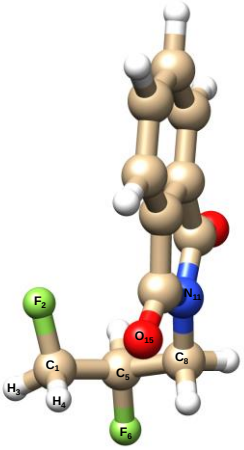	C_1 6.6 H_{10} 3.4 C_{14} -3.2	$F_2\cdots C_{14}$ 66.7 $F_2\cdots N_{11}$ -52.0 $C_1\cdots C_{14}$ -46.9 $F_2\cdots O_{15}$ -44.8	$F_2\cdots N_{11}$ 4.5 $C_1\cdots C_5$ -3.5

Table S8. Absolute (a.u) and relative $E_{\mathbf{14a\text{-}conf1}} - E_{\mathbf{14a\text{-}confi}}$ energies (kcal/mol) of the conformers optimize for **14a** at HF-D3/cc-pVTZ in gas-phase and in chloroform. Selected dihedral angles (º) and intramolecular distances (Å) are also included for the optimized structures (values in parentheses correspond to the solution structures). For the phenyl and the isoindoline-1,3-dione aromatic rings, the distance between the center of mass and the angle between the planes are also included.

	HF-D3/cc-pVTZ	**HF-D3/cc-pVTZ SMD**	**F_{23}-C_{22}-C_{25}=O_{26}**	**F_{23}-C_{22}-C_{19}-F_{20}**	**F_{20}-C_{19}-C_{16}-N_{13}**	**Aromatic rings**
14a-conf1	-1527.900462 (0.00)	-1527.938920 (0.00)	-179.4 (-177.7)	67.5 (66.4)	61.1 (61.2)	8.8/48.0 (8.9/43.7)
14a-conf2	-1527.901636 (0.74)	-1527.937246 (-1.05)	171.2 (169.0)	-58.4 (-58.8)	53.6 (56.2)	7.4/35.6 (7.4/39.3)
14a-conf3	-1527.898920 (-0.97)	-1527.934012 (-3.08)	147.7 (147.1)	-78.1 (-76.8)	55.3 (52.0)	5.2/15.6 (5.3/17.3)
14a-conf4	-1527.898530 (-1.21)	-1527.935687 (-2.03)	-178.3 (-177.5)	57.6 (59.7)	166.9 (170.6)	10.3/79.8 (10.3/83.9)
14a-conf5	-1527.897323 (-1.97)	-1527.935517 (-2.14)	177.1 (171.9)	-143.2 (-159.7)	71.0 (67.3)	5.1/12.1 (5.2/4.2)
14a-conf6	-1527.896251 (-2.64)	-1527.932337 (-4.13)	1.8 (2.0)	-153.8 (-154.0)	-162.1 (-162.5)	8.2/87.0 (8.2/77.4)
14a-conf7	-1527.894583 (-3.69)	-1527.930825 (-5.08)	-178.2 (-177.3)	-55.6 (-49.3)	40.0 (50.0)	6.9/86.2 (6.7/71.8)
14a-conf8	-1527.894558 (-3.70)	-1527.931927 (-4.39)	-147.4 (-146.8)	-45.2 (-45.0)	-47.0 (-52.9)	9.0/61.4 (8.7/55.2)
14a-conf9	-1527.894194 (-3.93)	-1527.934486 (-2.78)	177.9 (-179.5)	57.7 (59.7)	167.2 (171.3)	10.3/55.3 (10.3/54.7)
14a-conf10	-1527.893735 (-4.22)	-1527.934880 (-2.54)	176.4 (179.4)	66.2 (65.0)	61.2 (61.6)	9.2/51.6 (9.4/58.8)
14a-conf11	-1527.893705 (-4.24)	-1527.932785 (-3.85)	169.4 (175.5)	49.6 (54.4)	167.4 (170.7)	8.1/75.1 (8.9/79.6)

Table S8 (cont.)

	HF-D3/cc-pVTZ	HF-D3/cc-pVTZ SMD	F_{23}-C_{22}-C_{25}=O_{26}	F_{23}-C_{22}-C_{19}-F_{20}	F_{20}-C_{19}-C_{16}-N_{13}	Aromatic rings
14a-conf12	-1527.893302 (-4.49)	-1527.932785 (-3.85)	169.4 (168.4)	-58.6 (-56.6)	56.3 (59.8)	8.5/85.5 (8.3/74.7)
14a-conf13	-1527.893188 (-4.56)	-1527.932512 (-4.02)	174.6 (176.5)	47.4 (49.8)	-66.0 (-64.9)	8.1/48.8 (8.7/46.1)
14a-conf14	-1527.892694 (-4.87)	-1527.934433 (-2.82)	172.8 (178.0)	54.9 (59.5)	167.7 (171.9)	8.6/50.9 (10.2/55.8)
14a-conf15	-1527.890338 (-6.35)	-1527.928668 (-6.43)	-10.8 (-11.7)	-165.7 (-167.4)	44.3 (44.4)	9.9/60.5 (10.0/61.0)
14a-conf16	-1527.889986 (-6.57)	-1527.929768 (-5.74)	-12.4 (-14.4)	58.0 (55.8)	-171.9 (-170.1)	7.2/88.0 (7.2/86.4)
14a-conf17	-1527.888970 (-7.21)	-1527.928708 (-6.41)	-21.5 (-22.0)	48.4 (48.5)	-177.2 (-174.5)	5.7/72.4 (5.8/66.5)
14a-conf18	-1527.888613 (-7.44)	-1527.929018 (-6.21)	-16.4 (-16.4)	53.2 (51.6)	-173.7 (-172.5)	6.9/73.3 (6.8/75.2)
14a-conf19	-1527.887910 (-7.88)	-1527.928883 (-6.30)	-17.1 (-16.6)	43.8 (44.0)	-174.2 (-173.5)	6.1/66.6 (6.1/69.4)
14a-conf20	-1527.887650 (-8.04)	-1527.929098 (-6.16)	-17.7 (-18.6)	47.5 (46.1)	-175.9 (-174.2)	6.2/64.9 (6.3/65.5)

Figure S2. Ball-and-stick representation of the conformers optimized for **14a**.

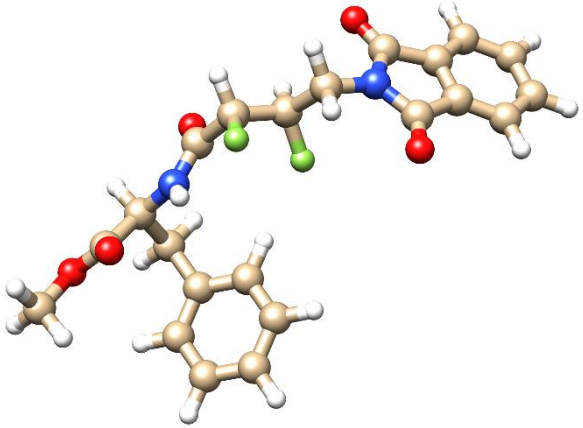

14a-conf1

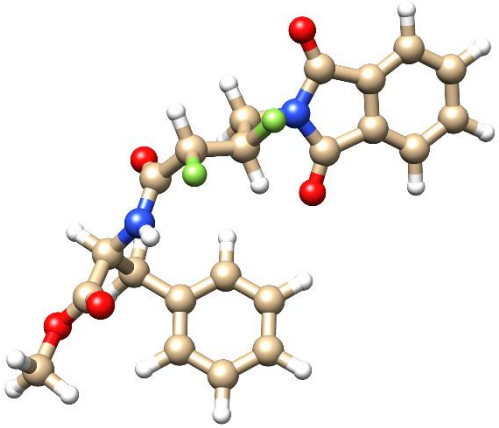

14a-conf2

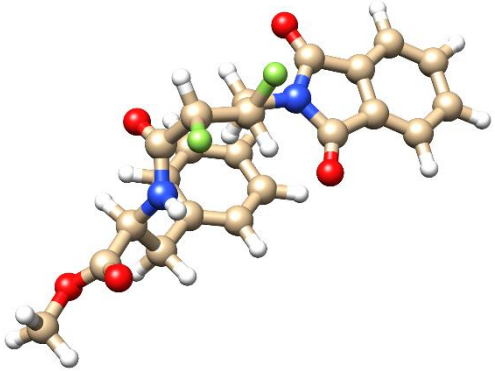

14a-conf3

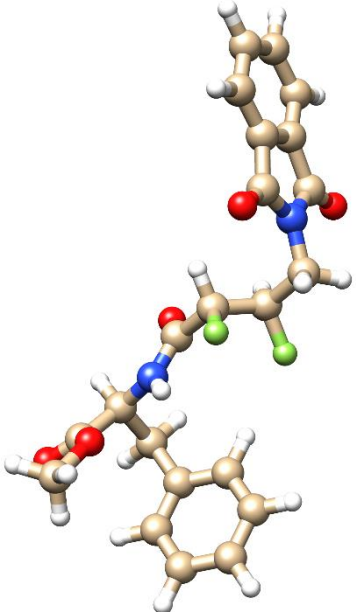

14a-conf4

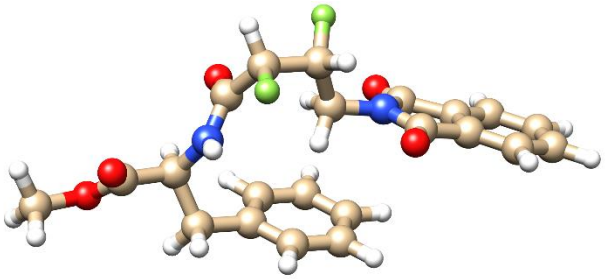

14a-conf5

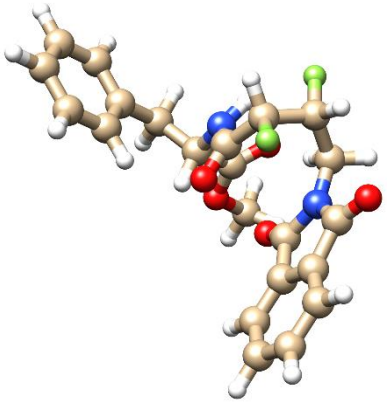

14a-conf6

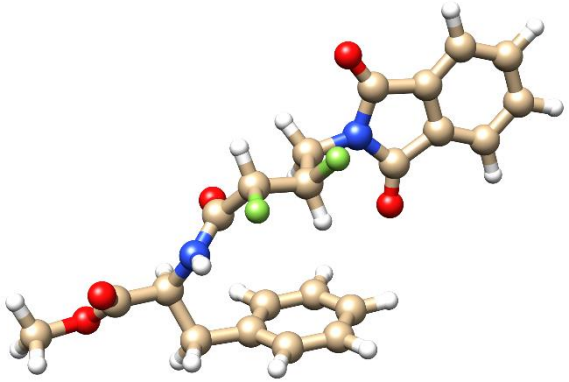

14a-conf7

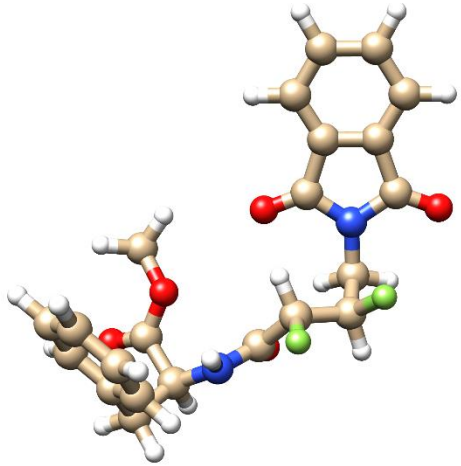

14a-conf8

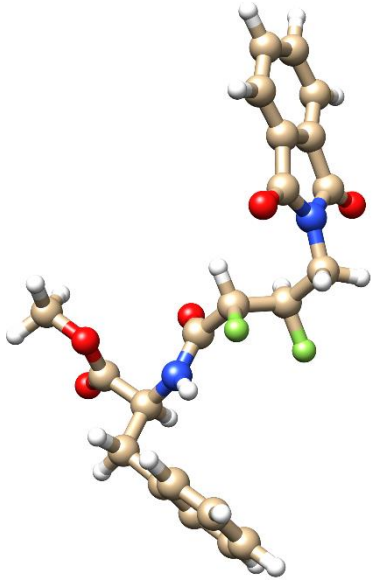

14a-conf9

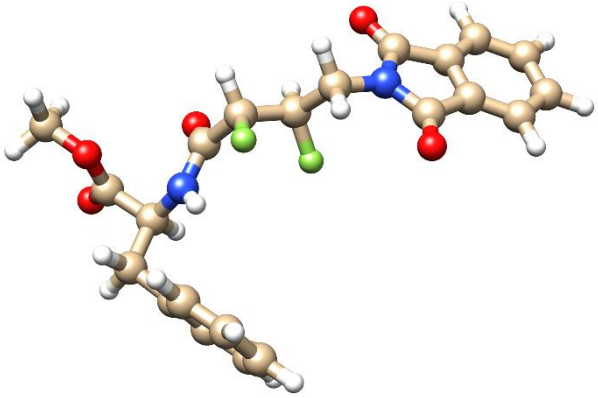

14a-conf10

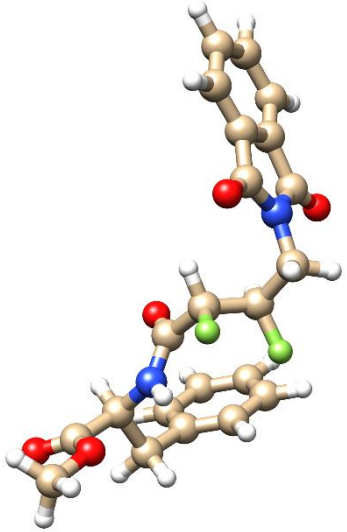

14a-conf11

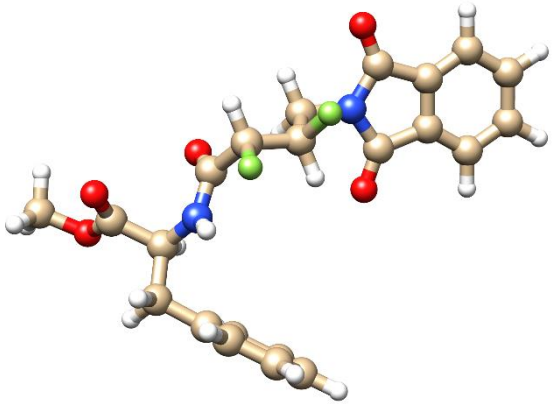

14a-conf12

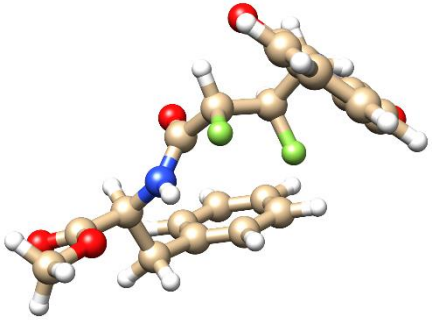

14a-conf13

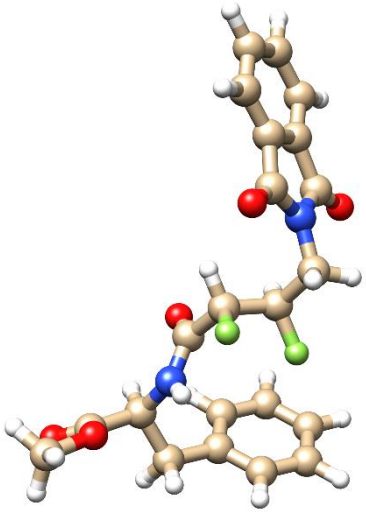

14a-conf14

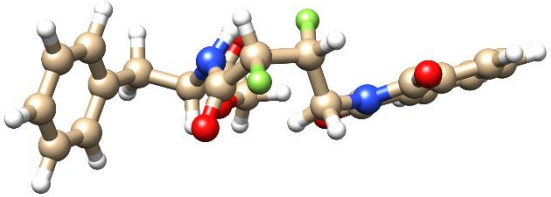

14a-conf15

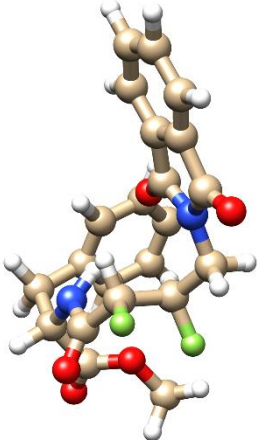

14a-conf16

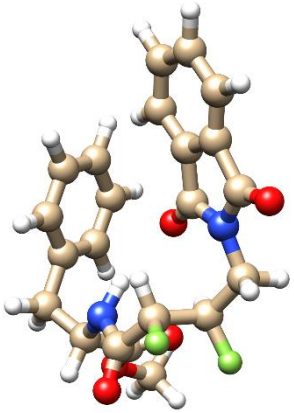

14a-conf17

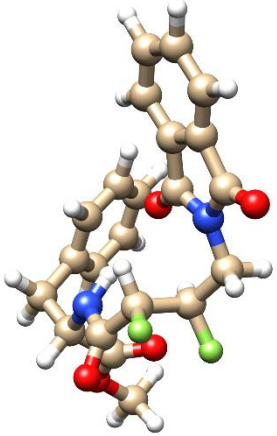

14a-conf18

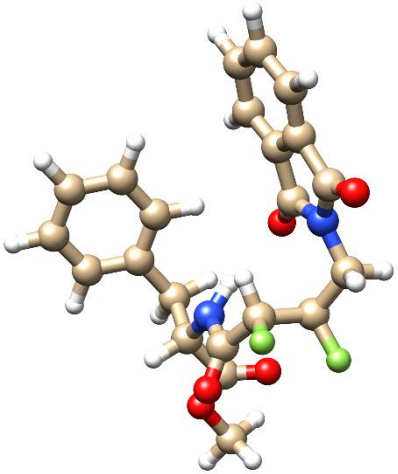

14a-conf19

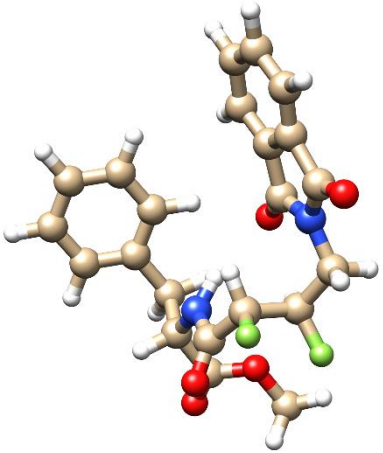

14a-conf20

Table S9. Absolute (a.u) and relative $E_{\mathbf{14b\text{-}conf1}}-E_{\mathbf{14b\text{-}confi}}$ energies (kcal/mol) of the conformers optimize for **14b** at HF-D3/cc-pVTZ in gas-phase and in chloroform. Selected dihedral angles (º) and intramolecular distances (Å) are also included for the optimized structures (values in parentheses correspond to the solution structures). For the phenyl and the isoindoline-1,3-dione aromatic rings, the distance between the center of mass and the angle between the planes are also included.

	HF-D3/cc-pVTZ	HF-D3/cc-pVTZ SMD	F_{23}-C_{22}-C_{25}=O_{26}	F_{23}-C_{22}-C_{19}-F_{20}	F_{20}-C_{19}-C_{16}-N_{13}	Aromatic rings
14b-conf1	-1527.902500 (0.00)	-1527.939296 (0.00)	178.6 (176.9)	-61.5 (-62.1)	-57.8 (-59.7)	5.1/9.4 (5.3/2.9)
14b-conf2	-1527.901093 (-0.88)	-1527.938076 (-0.76)	164.2 (163.8)	62.7 (62.8)	-59.5 (-57.6)	7.1/56.2 (7.2/55.6)
14b-conf3	-1527.900464 (-1.28)	-1527.937182 (-1.33)	-154.2 (-159.5)	-59.6 (-59.8)	65.2 (63.1)	6.0/36.2 (6.1/47.0)
14b-conf4	-1527.900032 (-1.55)	-1527.936010 (-2.06)	-161.5 (-164.3)	-60.5 (-60.9)	62.9 (62.0)	6.2/49.8 (6.2/52.7)
14b-conf5	-1527.896562 (-3.73)	-1527.933585 (-3.58)	151.5 (153.9)	-175.1 (178.2)	-63.9 (-62.4)	5.4/31.7 (6.2/29.4)
14b-conf6	-1527.895575 (-4.34)	-1527.931327 (-5.00)	173.3 (175.3)	62.7 (66.5)	166.5 (166.9)	9.7/60.8 (9.9/62.1)
14b-conf7	-1527.895159 (-4.61)	-1527.933710 (-3.50)	155.2 (152.6)	174.9 (171.8)	47.1 (54.3)	8.8/44.5 (9.3/54.2)
14b-conf8	-1527.894857 (-4.80)	-1527.932939 (-3.99)	-178.7 (173.3)	-63.3 (-65.2)	53.0 (51.4)	9.0/31.2 (9.1/31.2)
14b-conf9	-1527.894542 (-4.99)	-1527.935381 (-2.46)	-33.6 (-31.1)	71.8 (71.1)	-165.8 (-167.2)	7.5/47.1 (7.4/46.4)
14b-conf10	-1527.893634 (-5.56)	-1527.930076 (-5.78)	154.0 (153.0)	165.9 (166.6)	-178.9 (-176.8)	7.8/86.5 (7.7/86.6)
14b-conf11	-1527.892823 (-6.07)	-1527.933524 (-3.62)	176.2 (168.2)	-64.0 (-66.1)	52.1 (50.8)	9.2/88.7 (9.3/81.0)

Table S9 (cont.)

	HF-D3/cc-pVTZ	HF-D3/cc-pVTZ SMD	F_{23}-C_{22}-C_{25}=O_{26}	F_{23}-C_{22}-C_{19}-F_{20}	F_{20}-C_{19}-C_{16}-N_{13}	Aromatic rings
14b-conf12	-1527.892659 (-6.18)	-1527.932022 (-4.56)	-163.2 (160.9)	-149.5 (-176.1)	-52.0 (-66.5)	7.0/77.7 (5.3/39.6)
14b-conf13	-1527.892565 (-6.23)	-1527.930652 (-5.42)	158.8 (160.3)	-172.8 (-177.0)	-67.9 (-66.9)	4.9/41.4 (5.3/39.5)
14b-conf14	-1527.891884 (-6.66)	-1527.929878 (-5.91)	23.8 (21.6)	-63.2 (-61.4)	-78.1 (-77.9)	5.6/77.5 (5.8/74.6)
14b-conf15	-1527.890527 (-7.51)	-1527.929359 (-6.24)	-164.4 (-168.4)	-150.5 (-157.5)	-51.5 (-54.9)	6.9/78.9 (6.9/87.6)
14b-conf16	-1527.890134 (-7.76)	-1527.931522 (-4.88)	-23.7 (-15.4)	-71.5 (-69.7)	-67.2 (-83.9)	10.5/62.5 (9.1/84.0)
14b-conf17	-1527.888887 (-8.54)	-1527.928227 (-6.94)	165.5 (163.2)	-177.5 (179.9)	44.2 (51.1)	7.8/66.4 (8.0/77.2)
14b-conf18	-1527.888717 (-8.65)	-1527.928716 (-6.64)	-68.1 (-41.1)	176.8 (172.6)	45.9 (53.1)	8.8/86.2 (7.8/61.8)
14b-conf19	-1527.886233 (-10.21)	-1527.926181 (-8.23)	151.4 (152.5)	161.5 (164.2)	179.1 (-179.4)	11.2/57.8 (11.2/61.8)
14b-conf20	-1527.885198 (-10.86)	-1527.926237 (-8.19)	178.1 (161.1)	-148.2 (-176.8)	-56.1 (-59.3)	12.0/50.1 (11.9/86.0)

Figure S3. Ball-and-stick representation of the conformers optimized for **14b**.

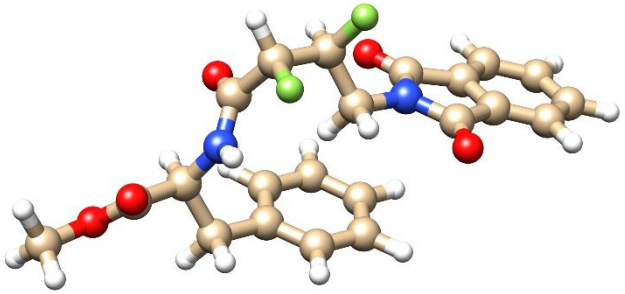

14b-conf1

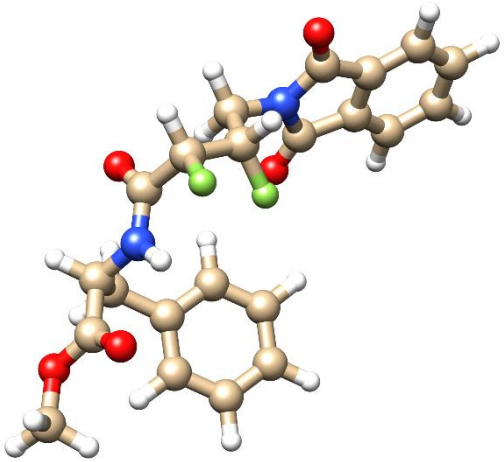

14b-conf2

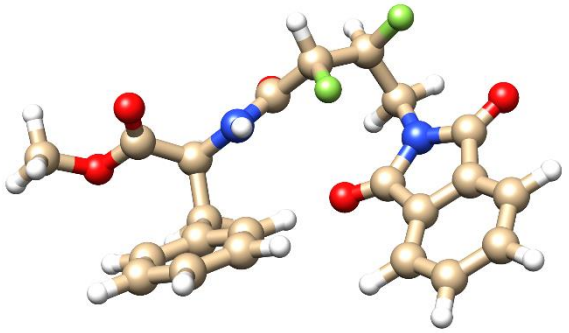

14b-conf3

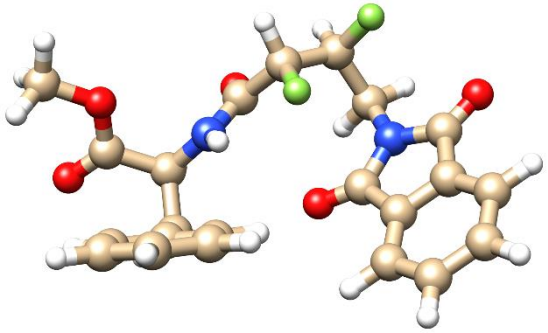

14b-conf4

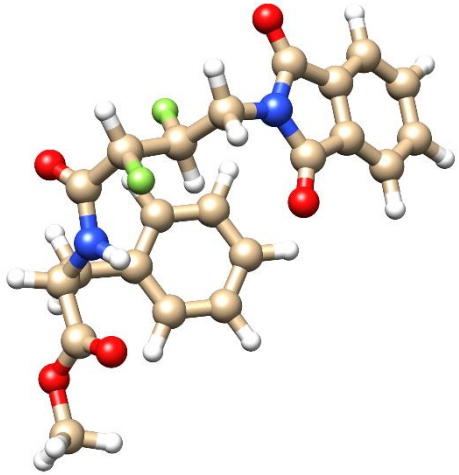

14b-conf5

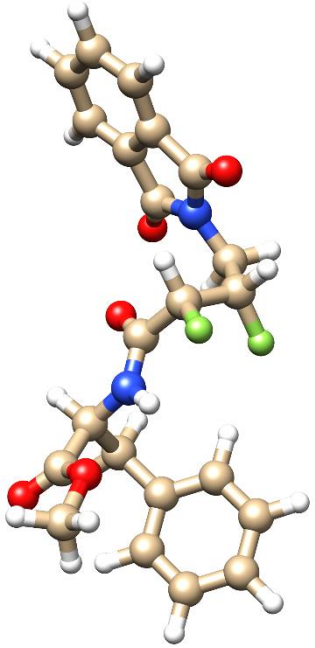

14b-conf6

.

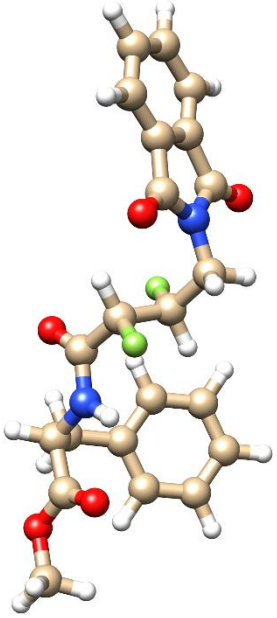

14b-conf7

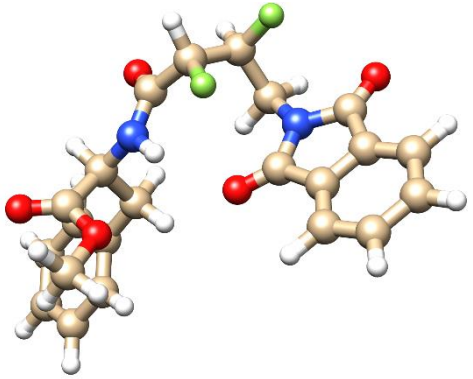

14b-conf8

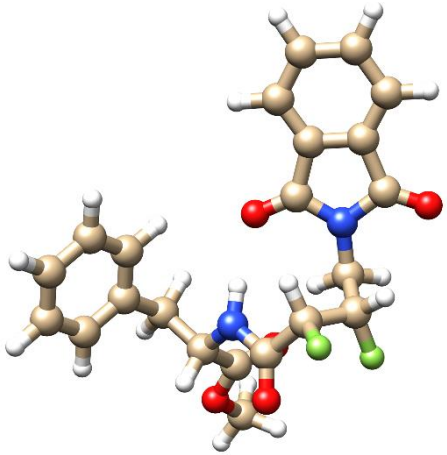

14b-conf9

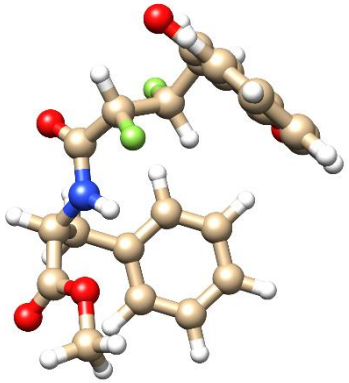

14b-conf10

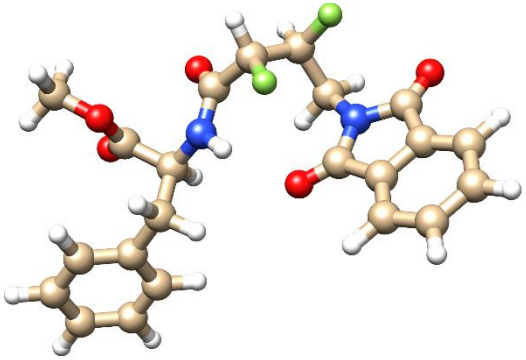

14b-conf11

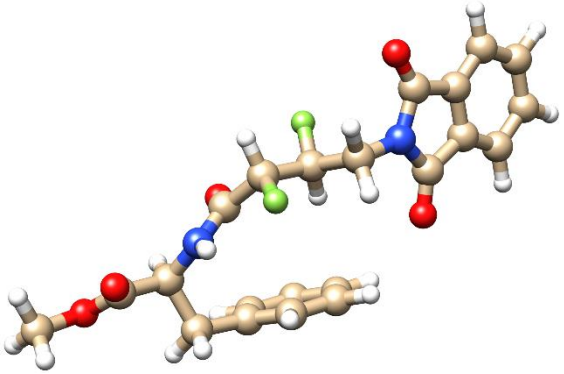

14b-conf12

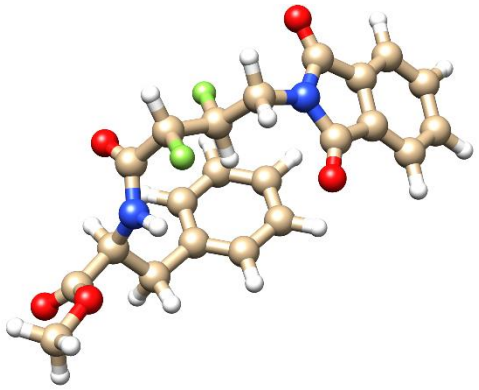

14b-conf13

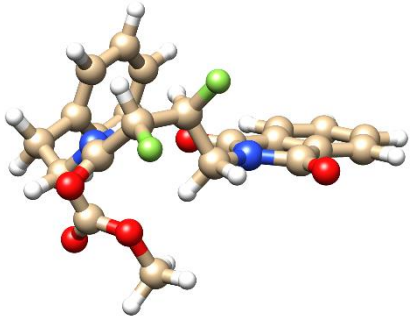

14b-conf14

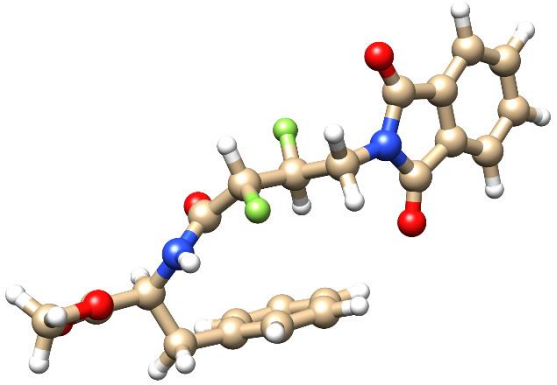

14b-conf15

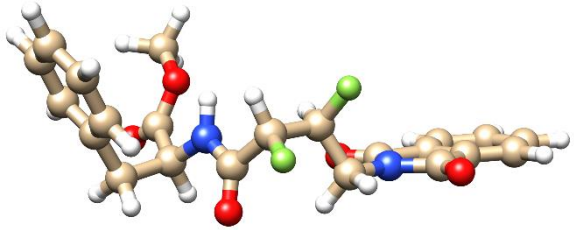

14b-conf16

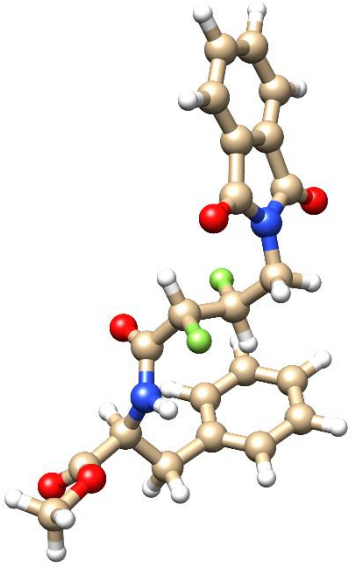

14b-conf17

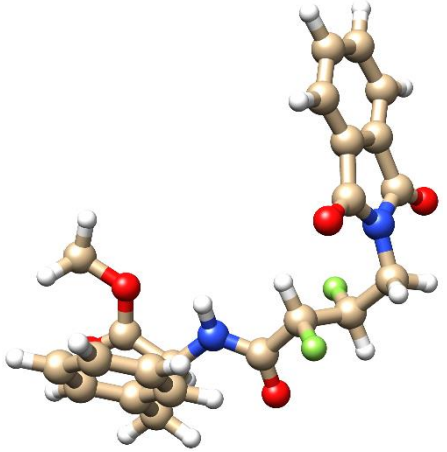

14b-conf18

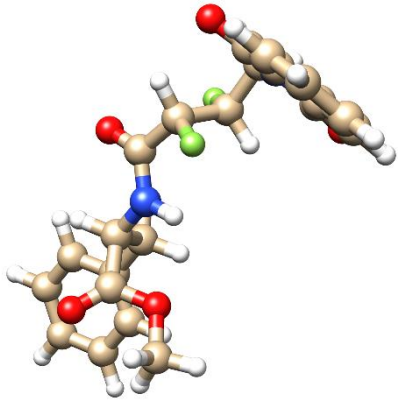

14b-conf19

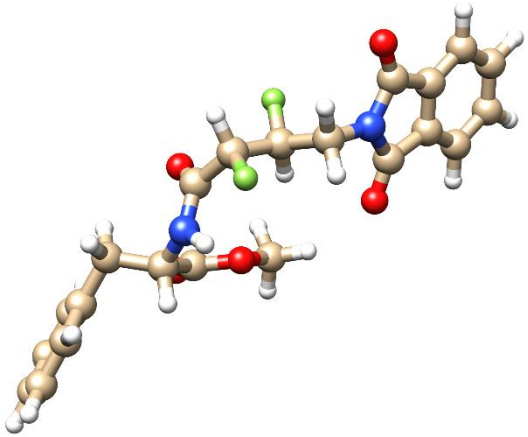

14b-conf20

Table S10. Estimated NMR coupling constants (*Hz*) between vicinal fluorine and hydrogen atoms around the C_{22}-C_{19} bond in selected conformers of the **14a** and **14b** compounds. Relative population of the different conformers at 300 K according to the Boltzmann distribution and the HF-D3/cc-pVTZ relative energies in chloroform. Coupling constants (*Hz*) obtained from the NMR spectra of **14a** and **14b** recorded in $CDCl_3$ at 300 K.

	$^3J_{FH}$	$^3J_{HF}$	P_i		$^3J_{FH}$	$^3J_{HF}$	P_i
14a-conf1	30.8	31.8	0.807	**14b-conf1**	30.8	8.1	0.704
14a-conf2	8.4	8.8	0.139	**14b-conf2**	6.6	31.7	0.197
14a-conf3	17.2	14.6	0.027	**14b-conf3**	31.3	10.4	0.076
14a-conf4	30.6	31.8	0.022	**14b-conf4**	31.6	10.5	0.022
14a-conf5	21.2	17.1	0.005	**14b-conf5**	5.2	3.9	0.002
Averaged	27.4	28.2	1.0	Averaged	26.1	13.0	1.0
NMR	27.0	28.9	--	NMR	23.0	21.4	--

Table S11. Largest differences in the atomic energies (kcal/mol) between the **14a-conf1** conformer and selected *i*-conformers.

$\Delta E = E_{14a\text{-}conf1} - E_i$	ΔE_{net}		$\Delta E_{\mathrm{int,clas}}^{A\cdots B}$		$\Delta E_{\mathrm{int,xc}}^{A\cdots B}$	
14a-conf2	C_{25}	11.4	$F_{20}\cdots C_{25}$	-43.9	$H_{17}\cdots O_{26}$	5.0
	H_{17}	-4.6	$F_{20}\cdots O_{26}$	29.2	$F_{20}\cdots H_{44}$	-3.2
	N_{27}	-4.6	$N_{13}\cdots O_{26}$	-28.3	$C_{16}\cdots O_{26}$	3.1
	C_{19}	-4.2	$F_{20}\cdots N_{27}$	28.0	$O_{12}\cdots H_{42}$	3.0
	C_{16}	3.8	$C_{19}\cdots C_{25}$	27.1	$C_{11}\cdots O_{12}$	-2.3
	O_{12}	-3.7	$O_{12}\cdots N_{27}$	-25.6	$O_{12}\cdots H_{44}$	2.3
	O_{26}	-3.5	$C_{11}\cdots N_{27}$	23.8	$H_{21}\cdots O_{26}$	-2.3
	C_{22}	-2.1	$O_{12}\cdots C_{45}$	23.0	$H_{18}\cdots F_{23}$	-2.0
			$N_{13}\cdots C_{25}$	22.7	$C_{19}\cdots C_{22}$	-1.9
			$C_{11}\cdots C_{25}$	-22.5	$C_{16}\cdots F_{23}$	-1.8
			$C_{14}\cdots O_{26}$	21.7	$F_{20}\cdots F_{23}$	1.8
14a-conf5	C_{25}	14.5	$N_{13}\cdots C_{25}$	33.2	$N_{27}\cdots H_{28}$	6.3
	N_{27}	10.6	$N_{13}\cdots N_{27}$	-29.6	$C_{19}\cdots C_{22}$	-5.5
	C_{19}	-10.1	$C_{14}\cdots C_{25}$	-28.3	$H_{18}\cdots O_{26}$	3.6
	C_{11}	-6.6	$C_{14}\cdots N_{27}$	28.3	$N_{13}\cdots C_{14}$	3.4
	H_{28}	6.4	$F_{20}\cdots N_{27}$	27.0	$O_{15}\cdots H_{18}$	-3.4
	H_{17}	-5.9	$N_{13}\cdots O_{26}$	-26.5	$O_{12}\cdots H_{18}$	3.3
	O_{26}	-5.8	$C_{25}\cdots N_{27}$	-25.9	$F_{20}\cdots H_{44}$	-3.3
			$F_{20}\cdots C_{25}$	-24.4	$C_{25}\cdots N_{27}$	-3.0
			$O_{15}\cdots N_{27}$	-23.9	$O_{26}\cdots H_{33}$	-2.6
			$O_{15}\cdots C_{25}$	23.7	$O_{26}\cdots H_{30}$	2.6
			$C_{11}\cdots N_{27}$	20.0	$N_{13}\cdots C_{39}$	2.6
14a-conf6	N_{27}	20.0	$C_{11}\cdots C_{45}$	-194.5	$N_{27}\cdots H_{28}$	8.0
	C_{25}	16.5	$O_{12}\cdots C_{45}$	194.1	$F_{23}\cdots O_{26}$	5.9
	O_{26}	-13.2	$C_{11}\cdots C_{25}$	-172.0	$F_{23}\cdots N_{27}$	-5.7
	C_{22}	-12.7	$C_{11}\cdots O_{46}$	136.5	$C_{19}\cdots C_{22}$	-4.5
	O_{12}	-11.0	$N_{13}\cdots C_{25}$	136.2	$H_{17}\cdots O_{46}$	4.3
	H_{28}	8.6	$C_{11}\cdots O_{26}$	135.6	$O_{26}\cdots H_{44}$	4.2
	H_{17}	-8.5	$O_{12}\cdots O_{46}$	-130.9	$C_{45}\cdots O_{46}$	-4.0
	C_{45}	-8.4	$O_{12}\cdots O_{47}$	-129.1	$C_{25}\cdots N_{27}$	-4.0
	F_{23}	-7.3	$C_{11}\cdots N_{27}$	127.5	$O_{12}\cdots O_{26}$	3.9
			$O_{12}\cdots C_{25}$	126.4	$C_{29}\cdots C_{31}$	3.7
			$C_{11}\cdots O_{47}$	125.9	$C_{16}\cdots H_{17}$	-3.4

Table S12. Equivalence between the filenames with the Cartesian coordinates for the HF/MP2 minima available as Supporting Information and the names of the compounds used in the text/Tables/Figures.

Filename	Compound	Filename	Compound
1_gauche_HF.xyz 1_gauche_MP2.xyz	**1**: 1,2-difluoroethane in gauche	1_anti_HF.xyz 1_anti_MP2.xyz	**1**: 1,2-difluoroethane in anti
2_gauche_HF.xyz 2_gauche_MP2.xyz	**2**: 2-fluoroethyl-acetate in gauche	2_anti_HF.xyz 2_anti_MP2.xyz	**2:** 2-fluoroethyl-acetate in anti
3_gauche_HF.xyz 3_gauche_MP2.xyz	**3**: 3-fluoropropanal in gauche	3_anti_HF.xyz 3_anti_MP2.xyz	**3:** 3-fluoropropanal in anti
4_gauche_HF.xyz 4_gauche_MP2.xyz	**4**: *N*-(2-fluoroethyl)acetamide in gauche	4_anti_HF.xyz 4_anti_MP2.xyz	**4**: *N*-(2-fluoroethyl)acetamide in anti
5_gauche_HF.xyz 5_gauche_MP2.xyz	**5**: 2-(2-fluoroethyl)isoindole-1,3-dione in gauche	5_anti_HF.xyz 5_anti_MP2.xyz	**5**: 2-(2-fluoroethyl)isoindole-1,3-dione in anti
6_gauche_HF.xyz 6_gauche_MP2.xyz	**6**: 2-fluoroethan-1-ammonium in gauche	6_anti_HF.xyz 6_anti_MP2.xyz	**6**: 2-fluoroethan-1-ammonium in anti
7_gauche_HF.xyz 7_gauche_MP2.xyz	**7**: 1-(2-fluoroethyl)pyridin-1-ium in gauche	7_anti_HF.xyz 7_anti_MP2.xyz	**7**: 1-(2-fluoroethyl)pyridine-1-ium in anti
8_trans_HF.xyz 8_trans_MP2.xyz	**8**: 1-fluoropropan-2-one in trans	8_cis_HF.xyz 8_cis_MP2.xyz	**8**: 1-fluoropropan-2-one in cis
9_trans_HF.xyz 9_trans_MP2.xyz	**9**: methyl-2-fluoroacetate in trans	9_cis_HF.xyz 9_cis_MP2.xyz	**9**: methyl-2-fluoroacetate in cis
10_trans_HF.xyz 10_trans_MP2.xyz	**10**: 2-fluoro-*N*-methylacetamide in trans	10_cis_HF.xyz 10_cis_MP2.xyz	**10**: 2-fluoro-*N*-methylacetamide in cis
11_g1g1_HF.xyz 11_g1g1_MP2.xyz	**11**: 1,2,3-trifluoropropane in g+/g+	11_g1g2_HF.xyz 11_g1g2_MP2.xyz	**11**: 1,2,3-trifluoropropane in g+/g-
11_g1anti_HF.xyz 11_g1anti_MP2.xyz	**11**: 1,2,3-trifluoropropane in g+/anti	11_g2g1_HF.xyz 11_g2g1_MP2.xyz	**11**: 1,2,3-trifluoropropane in g-/g+
11_g2anti_HF.xyz 11_g2anti_MP2.xyz	**11**: 1,2,3-trifluoropropane in g-/anti	11_antianti_HF.xyz 11_antianti_MP2.xyz	**11**: 1,2,3-trifluoropropane in anti/anti
12_g1trans_HF.xyz 12_g1trans_MP2.xyz	**12**: 2,3-difluoro-*N*-methylpropanamida in g+/trans	12_g2trans_HF.xyz 12_g2trans_MP2.xyz	**12**: 2,3-difluoro-*N*-methylpropanamida in g-/trans
12_antitrans_HF.xyz 12_antitrans_MP2.xyz	**12**: 2,3-difluoro-*N*-methylpropanamida in anti/trans	12_g1cis_HF.xyz 12_g1cis_MP2.xyz	**12**: 2,3-difluoro-*N*-methylpropanamida in g+/cis
12_anticis_HF.xyz 12_anticis_MP2.xyz	**12**: 2,3-difluoro-*N*-methylpropanamida in anti/cis	13_g1g1_HF.xyz 13_g1g1_MP2.xyz	**13**: 2-(2,3-difluoropropyl)isoindoline-1,3-dione in g+/g+
13_g1g2_HF.xyz 13_g1g2_MP2.xyz	**13**: 2-(2,3-difluoropropyl)isoindoline-1,3-dione in g+/g-	13_g1anti_HF.xyz 13_g1anti_MP2.xyz	**13**: 2-(2,3-difluoropropyl)isoindoline-1,3-dione in g+/anti
13_g2g1_HF.xyz 13_g2g1_MP2.xyz	**13**: 2-(2,3-fluoropropyl)isoindoline-1,3-dione in /g+	13_g2g2_HF.xyz 13_g2g2_MP2.xyz	**13**: 2-(2,3-difluoropropyl)isoindoline-1,3-dione in g-/g-
13_g2anti_HF.xyz 13_g2anti_MP2.xyz	**13**: 2-(2,3-difluoropropyl)isoindoline-1,3-dione in g-/anti	13_antig1_HF.xyz 13_antig1_MP2.xyz	**13**: 2-(2,3-difluoropropyl)isoindoline-1,3-dione in anti/g+
13_antig2_HF.xyz 13_antig2_MP2.xyz	**13**: 2-(2,3-difluoropropyl)isoindoline-1,3-dione in anti/g-	13_antianti_HF.xyz 13_antianti_MP2.xyz	**13**: 2-(2,3-difluoropropyl)isoindoline-1,3-dione in anti/anti
14a_conf1_HF.xyz	**14a-conf1**	14a_conf2_HF.xyz	**14a-conf2**
14a_conf5_HF.xyz	**14a-conf5**	14a_conf6_HF.xyz	**14a-conf6**

Table S13. IQF energy components for the energy difference (kcal/mol) between the *gauche/anti* confomers analyzed for 1,2-difluoroethane at different levels of theory. Two-fragment partitioning scheme (P=CH_2F- and Q=-CH_2F) is assumed for the system. Geometrical changes in distances (Å) and angles (º) between both conformers (*gauche-anti*) are also included.

$\Delta E = E_{gauche} - E_{anti}$	Δq^P	ΔE^P_{net}	ΔE^Q_{net}	$\Delta E_{int,disp}$	$\Delta E_{int,xc}$	$\Delta E_{int,class}$	ΔE_{IQA} (ΔE)[a]	C-C	C-F	F-C-C	IQA wall time [b]
HF-D3/cc-pVTZ	0.00	0.6	0.4	0.0	-3.5	2.1	-0.5 (-0.3)	-0.009	-0.002	2.2	24
B3LYP-D3/cc-pVTZ [c]	0.00	1.2	1.4	0.0	-5.8	2.2	-1.0 (-0.9)	-0.013	-0.002	2.5	26
MP2/cc-pVTZ [d]	0.00	0.3	0.3	-	-4.2	2.4	-1.2 (-0.8)	-0.012	-0.002	2.3	1348

(a) ΔE_{IQA}=IQA-reconstructed energy difference; ΔE= Exact energy difference at the corresponding level of theory. The difference between ΔE_{IQA} and ΔE is due to the numerical errors in the IQA calculations.

(b) Wall time in min of the IQA calculations running on a 12-core Xeon platform.

(c) The total energy of the Khon-Sham DFT energy is recovered with IQA using the scaling technique as described in Francisco, E.; Casals-Sainz, J. L.; Rocha-Rinza, T. and Martín Pendás, A. *Theoretical Chemistry Accounts* **2016**, 135.

(d) The MP2 correlation energy is expressed as $E_{corr} = \sum_{iajb} t_{ij}^{ab} \left(ia | jb \right)$ where t_{ij}^{ab} are the MP2 amplitudes, *(iajjb)* are two electron integrals in the molecular orbital basis (MO) (Mulliken convention) and *i, j* and *a, b* refer to occupied and virtual orbitals, respectively. The t_{ij}^{ab} amplitudes are obtained using a locally modified copy of the PySCF code by performing a single-point MP2/cc-pVTZ calculation on the corresponding optimized geometry. The MP2-correlated IQA calculations are also performed with the PROMOLDEN code. For further details on the correlated-IQA calculations see Casals-Sainz, J.L. Costales-Castro, A; Francisco, E. and Martín-Pendás, A. *Molecules* **2019**, *24*, 2204. For PYSCF see: Sun, Q.; Berkelbach, T.C.; Blunt, N.S.; Booth, G.H.; Guo, S.; Li, Z.; Liu, J.; McClain, J.D.; Sayfutyarova, E.R.; Sharma, S.; et al. *PySCF: The Python-based simulations of chemistry framework*. *Wiley Interdiscip. Rev. Comput. Mol. Sci.* **2018**, *8*, e1340.

Short comment on the results of Table S13

The three levels of theory predict similar geometrical changes upon the *anti→gauche* conformational change. The classical electrostatic penalty of the gauche conformation ($\Delta E_{\text{int,class}}$~2.1-2.4 kcal/mol) is also quite similar among the three computational approaches. They coincide again in predicting a significant quantum mechanical stabilization ($\Delta E_{int,xc}$) of the *gauche* conformer, although the B3LYP-based energy (-5.8 kcal/mol) is significantly larger in absolute value than the MP2/HF ones (-4.2/-3.5). B3LYP-D3 also differs in the relative importance of the fragment net energy changes (ΔE^{P}_{net} , ΔE^{Q}_{net} > 1 kcal/mol), the HF-D3 and MP2 values being closer to each other. Overall, we see that, with respect to HF-D3, inclusion of the MP2 dynamical correlation does not alter the qualitative changes of the IQF energy terms and has only a small quantitative impact. Note also that the MP2-IQA calculations are computationally very demanding (~10^2 more expensive than HF-IQA) so that they cannot performed on large molecular systems.